

Palmprint identification using feature-level fusion

Adams Kong^{a, b}, David Zhang^{a, *}, Mohamed Kamel^b

^aDepartment of Computing, Biometric Research Center, The Hong Kong Polytechnic University, Hung Hom, Kowloon, Hong Kong

^bPattern Analysis and Machine Intelligence Lab, University of Waterloo, Ont., Canada N2L 3G1

Received 15 September 2004; received in revised form 30 June 2005; accepted 11 August 2005

Abstract

In this paper, we propose a feature-level fusion approach for improving the efficiency of palmprint identification. Multiple elliptical Gabor filters with different orientations are employed to extract the phase information on a palmprint image, which is then merged according to a fusion rule to produce a single feature called the Fusion Code. The similarity of two Fusion Codes is measured by their normalized hamming distance. A dynamic threshold is used for the final decisions. A database containing 9599 palmprint images from 488 different palms is used to validate the performance of the proposed method. Comparing our previous non-fusion approach and the proposed method, improvement in verification and identification are ensured.

© 2005 Pattern Recognition Society. Published by Elsevier Ltd. All rights reserved.

Keywords: Palmprint; Biometrics; Fusion; Security; Zero-crossing

1. Introduction

Biometric personal identification/verification has long been a widely studied topic. Various technologies have been proposed and implemented, including iris, fingerprint, hand geometry, voice, face, signature and retina identification/verification [1] technologies. Each of these has its own strengths and weaknesses. Currently, hand-based biometric technologies such as fingerprint verification and hand geometry verification most appeal to the biometric identification market, with the International Biometric Group reporting that hand-based biometrics constitute 60% of the total market share as of 2001.

Automatic fingerprint verification is the most mature biometric technology, having been studied for more than 25 years. Currently, fingerprint authentication handles clear fingerprints very well but, because of skin problems or the nature of their work, around 2% of the population are unable to provide clear fingerprint images [2]. Consequently, many researchers continue to develop new scanning

technologies, preprocessing algorithms, feature representations, post-processing approaches, and classifiers to resolve problems arising from unclear fingerprint images.

Another popular, hand-based biometric technology is hand geometry [3]. Hand geometry uses geometric information from our hands for personal verification. Simple hand features, however, provide limited information, with the result that hand geometry is not highly accurate. To overcome problems in the hand-based biometric technologies, Zhang and Shu [4] proposed another hand-based biometric for use in personal identification/verification, the palmprint. The palmprint, the large inner surface of a hand, contains many line features such as principal lines, wrinkles, and ridges. Because of the large surface and the abundance of line features, we expect palmprints to be robust to noise and to be highly individual.

1.1. Previous work

Palmprint is a relatively new biometric technology. Previous researchers were mostly interested in inked palmprint images, in which lines and points were considered as useful features for representing palmprints [4,5]. Recently, more researchers have been working on inkless palmprint images

* Corresponding author. Tel.: +1 852 2766 7271; fax: +1 852 2774 0842.
E-mail address: csdzhang@comp.polyu.edu.hk (D. Zhang).

captured using a special palmprint scanner or a general digital scanner [6–8].

Biometric Research Centre at The Hong Kong Polytechnic University has developed a special palmprint scanner for acquiring high-quality palmprint images. The details of this palmprint scanner have been described in Ref. [7]. In addition to capture device, our group has also implemented various line-, texture-, and component-based approaches [7,9,10]. A promising result was obtained from a texture-based approach called PalmCode, reported in Ref. [7]. This approach exploited zero-crossing information on a palmprint image.

1.2. Motivation

As the proposed method has been developed with reference to PalmCode, we begin with a short review of the concept, in which

1. an adjusted circular Gabor filter is applied to the preprocessed palmprint images,
2. the signs of the filtered images are coded as a feature vector, and
3. two PalmCodes are measured using the normalized hamming distance.

Detailed implementations of PalmCode and the preprocessed palmprint image are discussed in Ref. [7]. Figs. 1(d)–(i) show three PalmCodes derived from the three different palms in Figs. 1(a)–(c). We can observe that the PalmCodes from the different palms are similar, having many 45° streaks. Intuitively, we might conclude that such structural similarities in the PalmCodes of different palms would reduce the individuality of PalmCodes and the performance of the palmprint identification system.

To reduce the correlation between PalmCodes, in this paper, we develop a fusion rule to select one of elliptical Gabor filters for coding the phase information. To further enhance the performance of the system, we replace the fixed threshold used in PalmCode by a dynamic threshold for the final decisions.

1.3. System overview

Our palmprint identification system consists of two parts: a palmprint scanner for on-line palmprint image acquisition and an algorithm for real-time palmprint identification. The system structure is illustrated in Fig. 2. The four main steps in our system are as follows:

- (1) Transmit a palmprint image to a computer from our palmprint scanner.
- (2) Determine the two key points between the fingers and extract the central parts based on the coordinate system established by the key points. As a result, different palmprint images are aligned.

- (3) Convolute the central parts using a number of Gabor filters. Merge the filter outputs, then code the phases as a feature vector called Fusion Code.
- (4) Use the normalized hamming distance to measure the similarity of two Fusion Codes and use a dynamic threshold for the final decision.

In this paper, we employ our previous preprocessing algorithm to segment the central parts of palmprints [7]. The proposed method will directly operate on the central parts of palmprints.

This paper is organized as follows. Section 2 presents the step-by-step implementation of Fusion Codes. Section 3 presents the bitwise hamming distance for matching two Fusion Codes and the dynamic threshold for final decision. Section 4 provides a series of experimental results including, verification, identification and computation time. Section 5 discusses the assumption for the development of the dynamic threshold. Section 6 offers our concluding remarks.

2. Implementation of Fusion Code

2.1. Filtering

First, the preprocessed palmprint image is passed to a Gabor filter bank. The filter bank contains a number of Gabor filters, which have the following general formula:

$$G(x, y, \theta, u, \sigma, \beta) = \frac{1}{2\pi\sigma\beta} \exp \left\{ -\pi \left(\frac{x'^2}{\sigma^2} + \frac{y'^2}{\beta^2} \right) \right\} \exp(2iux'), \quad (1)$$

where $x' = (x - x_0) \cos \theta + (y - y_0) \sin \theta$, $y' = -(x - x_0) \sin \theta + (y - y_0) \cos \theta$, (x_0, y_0) is the center of the function, u is the radial frequency in radians per unit length and θ is the orientation of the Gabor function in radians. σ and β are the standard deviations of the elliptical Gaussian along x and y axes, respectively. As in the implementation of PalmCode, the Gabor filters are adjusted to zero DC (direct current). The parameter θ in the Gabor filters is $j\pi/v$, where $j = 0, 1, \dots, v - 1$ and v is the total number of Gabor filters in the bank. The other parameters are optimized for d' index defined as $d' = |\mu_1 - \mu_2| / \sqrt{(\sigma_1^2 + \sigma_2^2)/2}$, where μ_1 and μ_2 are the means of genuine and impostor distributions, respectively, and σ_1 and σ_2 are their standard deviations. For convenience, we use G_j , to represent the Gabor filters.

2.2. Fusion rule design and feature coding

The filtered images contain two kinds of information: magnitude M_j and phase P_j , which are defined as

$$M_j(x, y) = \sqrt{G_j * I(x, y) \times \overline{G_j * I(x, y)}} \quad (2)$$

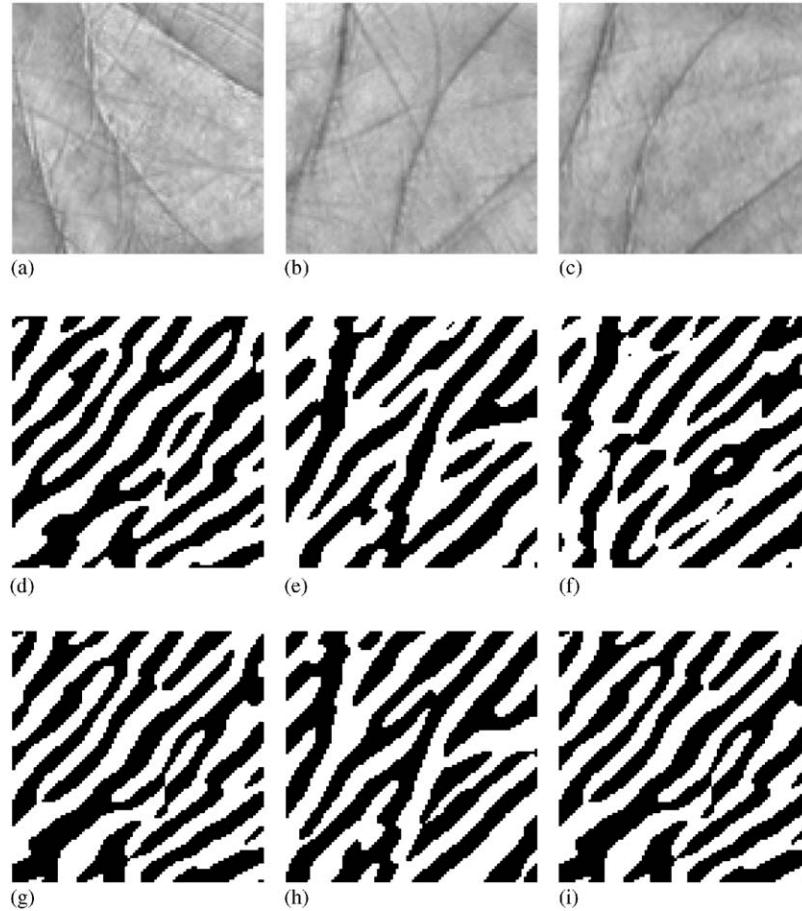


Fig. 1. Three typical samples of PalmCodes: (a)–(c) original images, (d)–(f) real parts of PalmCodes, (g)–(i) imaginary parts of PalmCode.

and

$$P_j(x, y) = \tan^{-1} \left(\frac{i(\overline{G_j * I(x, y)} - G_j * I(x, y))}{G_j * I(x, y) + \overline{G_j * I(x, y)}} \right), \quad (3)$$

where “ $\overline{\quad}$ ” represents complex conjugate, “ $*$ ” is an operator of convolution and I is a preprocessed palmprint image. Because of the zero DC Gabor filters, both phase and magnitude are independent of the DC of the image. DC relies on the brightness of the capturing environment. Phase is also independent of the contrast of the image but the magnitude is not. These properties can be observed from the following equations.

Let AI be a preprocessed image, where A , a positive number, controls the contrast of the image. The magnitude and the phase of the filtered palmprint image are:

$$AM_j(x, y) = \sqrt{G_j * AI(x, y) \times \overline{G_j * AI(x, y)}} \quad (4)$$

and

$$P_j(x, y) = \tan^{-1} \left(\frac{i(\overline{G_j * AI(x, y)} - G_j * AI(x, y))}{G_j * AI(x, y) + \overline{G_j * AI(x, y)}} \right), \quad (5)$$

respectively. As a result, since the PalmCode only uses the phase information, it is stable for two properties: variation in the contrast, and the DC of palmprint images. To design a fusion coding scheme inheriting these two properties, we employ the magnitude for fusion and the phase for the final feature. Thus, we propose a fusion rule:

$$k = \arg \max_j (M_j(x, y)) \quad (6)$$

and coding equations:

$$(h_r, h_i) = (1, 1) \quad \text{if } 0 \leq P_k(x, y) < \pi/2, \quad (7)$$

$$(h_r, h_i) = (0, 1) \quad \text{if } \pi/2 \leq P_k(x, y) < \pi, \quad (8)$$

$$(h_r, h_i) = (0, 0) \quad \text{if } \pi \leq P_k(x, y) < 3\pi/2, \quad (9)$$

$$(h_r, h_i) = (1, 0) \quad \text{if } 3\pi/2 \leq P_k(x, y) < 2\pi, \quad (10)$$

where h_r and h_i are bits in the real and the imaginary parts of the Fusion Code. A Fusion Code is illustrated in Fig. 3, which is generated by two elliptical Gabor filters.

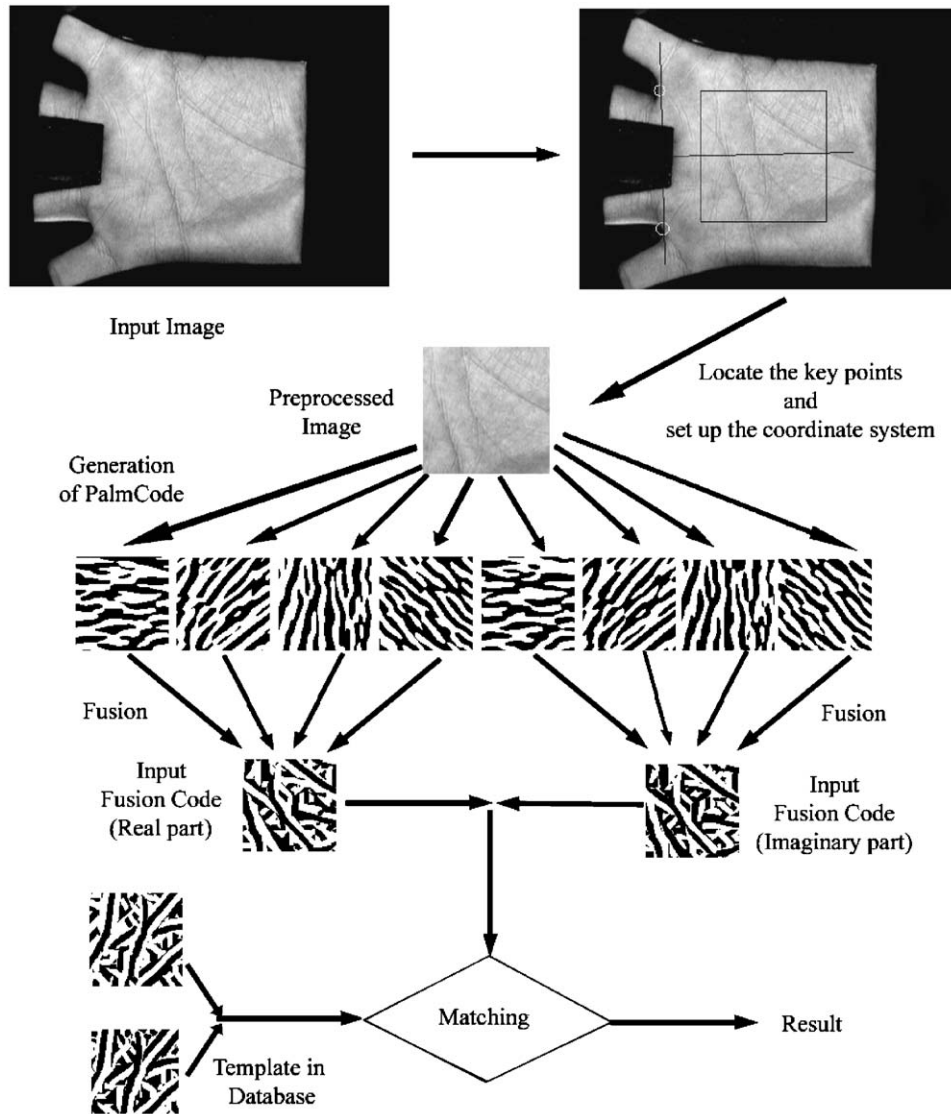


Fig. 2. Block diagram of our palmprint identification system.

3. Comparisons of Fusion Codes

In terms of the feature format, the proposed Fusion Code is exactly the same as that of the PalmCode. Consequently, the normalized hamming distance for the PalmCode is still useful for the Fusion Code. If we are given two data sets, a matching algorithm would determine the degree of similarity between them. To describe the matching process clearly, we use a feature vector to represent image data that consists of two feature matrices, a real one and an imaginary one. A normalized hamming distance is adopted to determine the similarity measurement for palmprint matching. Let P and Q be two palmprint feature vectors. The normalized hamming distance can be described as

where $P_R(Q_R)$, $P_I(Q_I)$ and $P_M(Q_M)$ are the real part, the imaginary part, and the mask of $P(Q)$, respectively. The mask is used to denote the non-palmprint pixels such as the boundary of the device which result from incorrect placement of user's hand. The result of the Boolean operator XOR (\otimes) is equal to zero, if and only if the two bits, $P_{R(I)}(i, j)$, are equal to $Q_{R(I)}(i, j)$. The symbol \cap represents the AND operator, and the size of the feature matrices is $N \times N$. It is noted that s is between 1 and 0. For the best matching, the normalized hamming should be zero. Because of imperfect preprocessing, we need to translate one of the features vertically and horizontally and match again. The ranges of the vertical and the horizontal translations are defined from

$$s = \frac{\sum_{i=1}^N \sum_{j=1}^N P_M(i, j) \cap Q_M(i, j) \cap ((P_R(i, j) \otimes Q_R(i, j) + P_I(i, j) \otimes Q_I(i, j)))}{2 \sum_{i=1}^N \sum_{j=1}^N P_M(i, j) \cap Q_M(i, j)}, \quad (11)$$

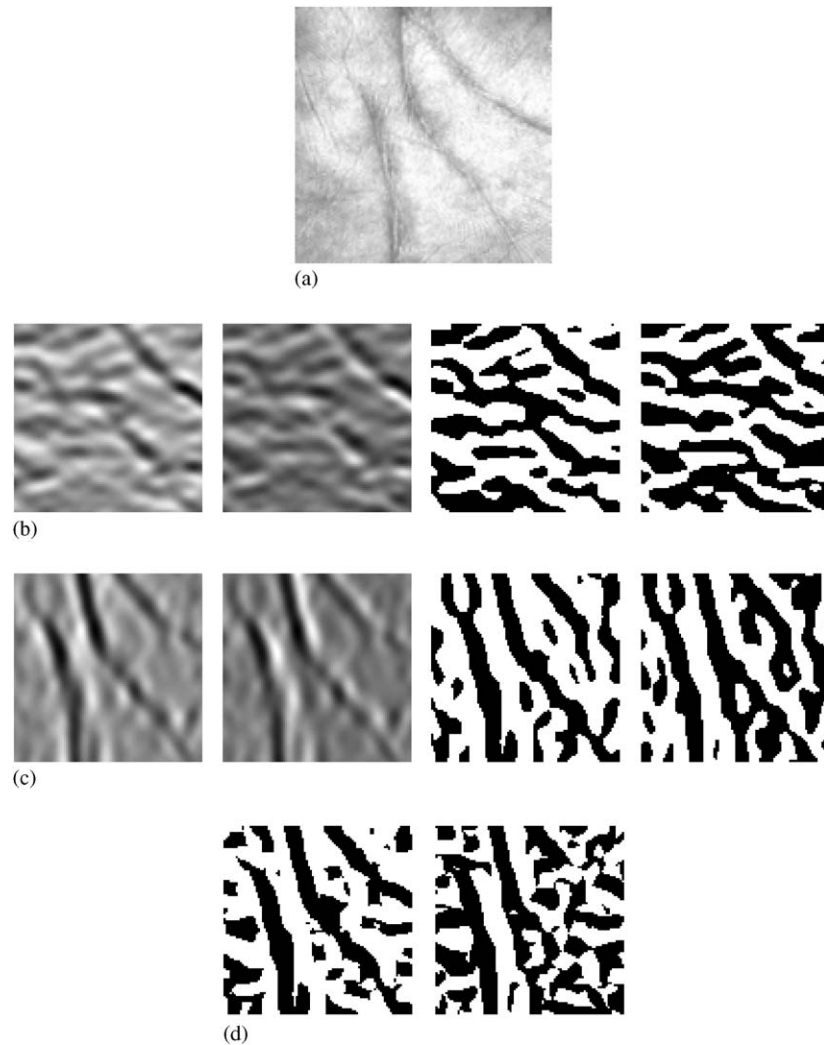


Fig. 3. Procedure of how the Fusion Code is generated: (a) original palmprint image, (b) and (c) real parts (Column 1) and imaginary parts (Column 2) of the filtered images, and real parts (Column 3) and imaginary parts (Column 4) of PalmCodes and (d) Fusion Code.

−2 to 2. The minimum s value obtained from the translated matching is treated as the final matching score.

In the original PalmCode, we use a fixed threshold to make the final decision. If the minimal translated matching score is greater than the fixed threshold, the system rejects the statement that two PalmCodes are from the same palm; otherwise, the system accepts it. When the effective matched bits are different, the fixed threshold has different statistical confidences for different decisions. To take into account this point, we propose the following dynamic threshold:

$$t_d = \mu_s - (\mu_s - t_s) \times \sqrt{m/2048}, \quad (12)$$

where μ_s is the mean of the imposter distribution without considering translated matching, t_s is a predefined threshold and m is the number of effective matched bits. Directly using Eq. (12) for real-time processing is not effective since it requires several operators and a function call for the square

root. To solve this problem, we pre-compute all the values of t_d and store them in a look up table.

Eq. (12) is derived based on the assumption that the imposter matching score, s follows binomial distribution, $B(n, \mu_s)$, where n is the degrees-of-freedom and μ_s is the probability of success in each Bernoulli trial. Mathematically, the distribution is defined as

$$f(s) = \frac{n!}{x!(n-x)!} \mu_s^x (1 - \mu_s)^{n-x}, \quad (13)$$

where x is the integer part of $n \times s$. In Section 5, we will discuss this assumption. Let s_1 be an imposter matching score and the corresponding number of effective matched bits is m . We also assume that s_1 follows $B(a, \mu_s)$ and its degrees-of-freedom, a is proportional to m . If n and a are large enough, we can use normal distributions to approximate the binomial distributions and obtain the following

equation:

$$\int_{-\infty}^{\frac{t_s - \mu_s}{\sqrt{\mu_s(1-\mu_s)/n}}} \frac{s - \mu_s}{\sqrt{\mu_s(1-\mu_s)/n}} ds = \int_{-\infty}^{\frac{t_d - \mu_s}{\sqrt{\mu_s(1-\mu_s)/a}}} \frac{s_1 - \mu_s}{\sqrt{\mu_s(1-\mu_s)/a}} ds_1. \quad (14)$$

Since both $(s - \mu_s)/\sqrt{\mu_s(1-\mu_s)/n}$ and $(s_1 - \mu_s)/\sqrt{\mu_s(1-\mu_s)/a}$ follow standard normal distributions, we have

$$\frac{t_s - \mu_s}{\sqrt{\mu_s(1-\mu_s)/n}} = \frac{t_d - \mu_s}{\sqrt{\mu_s(1-\mu_s)/a}}. \quad (15)$$

Simplifying Eq. (15) and using the assumption that the degrees-of-freedom is proportional to the number of the effective matched bits, we can obtain Eq. (12). For matching two non-translated and clear palmprints, the number of matched bits should be 2048. IrisCode also uses a similar dynamic threshold but all the mathematical derivations have not been disclosed clearly [11].

4. Experimental results and comparisons

4.1. Palmprint database

We collected palmprint images from 284 individuals using our palmprint capture device as described in Ref. [7]. In this dataset, 186 people are male, and the age distribution of the subjects is: about 89% are younger than 30, about 10% are aged between 30 and 50, and about 1% are older than 50. The palmprint images were collected on two separate occasions, at an interval of around two months. On each occasion, the subject was asked to provide about 10 images each of the left palm and the right palm. Therefore, each person provided around 40 images, resulting in a total number of 11,074 images from 568 different palms in our database. The average time interval between the first and second occasions was 73 days. The maximum and the minimum time intervals were 340 days and 1 day, respectively. The size of all the test images used in the following experiments was 384×284 with a resolution of 75 dpi. We divided the database into two datasets, training and testing. Testing set contained 9599 palmprint images from 488 different palms and training set contained the rest of them. We use only the training set to adjust the parameters of the Gabor filters. All the experiments were conducted on the testing set. We should emphasize that matching palmprints from the same sessions was not counted in the following experiments. In other words, the palmprints from the first session were only matched with the palmprints from the second session. A matching is counted as a genuine matching if two palmprint images are from the same palm; otherwise it is counted as an imposter matching. Number of genuine and imposter matching are 47,276 and 22,987,462, respectively. In the following, we use receiver operating characteristic

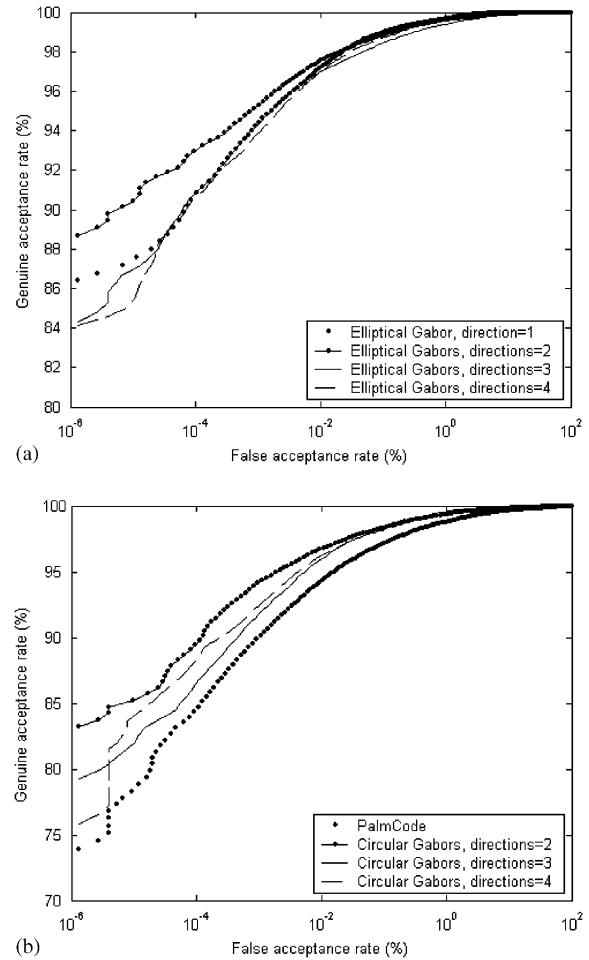


Fig. 4. Comparisons between different numbers of filters used in fusion, (a) elliptical Gabor filters and (b) circular Gabor filters.

(ROC) curve, which is a plot of the genuine acceptance rate against the false acceptance rate for all possible operating points for comparisons.

4.2. Comparisons of different types and different numbers of Gabor filters

In this experiment, different numbers of elliptical and circular Gabor filters are examined. Using d' index as an objective function, we optimize the parameters in the elliptical Gabor filters. For the circular Gabor filters, we use the previous parameters [7,12] for these comparisons. Fig. 4(a) shows the four ROC curves obtained from elliptical Gabor filters. Each of the ROC curve represents different numbers of Gabor filters used in the fusion rule. Fig. 4(b) shows the results obtained from the circular Gabor filters. In this test, we still use the static threshold, rather than the dynamic threshold. According to Fig. 4, we have two observations. (1) The elliptical Gabor filters perform better than the circular Gabor filters. (2) Using two filters for fusion is the

best choice for both cases. We can easily understand the first observation. The elliptical Gabor filters have more parameters so that they can be well tuned for palmprint features. The reason for the second observation is not obvious. Therefore, we conduct another set of experiments. In this set of experiments, we consider only the elliptical case. First of all, we plot the imposter distributions without considering translated matching in Fig. 5(a). We can see that the imposter distributions from two to four filters are very similar. Their means, μ_s are 0.497 and standard deviations, σ_s are around 0.0258. However, the imposter distribution from a single filter has a relatively large variance. If we use binomial distribution to model the imposter distributions, the imposter distributions from two to four filters have around 370 degrees-of-freedom. However, the imposter distribution from the single filter only has 250 degrees-of-freedom. The degrees-of-freedom are estimated by $\mu_s(I - \mu_s)/\sigma_s^2$. These values demonstrate that using more than two filters cannot improve the imposter distributions but increasing number of filters from one to two can get a great improvement. Although increasing number of filters can reduce the variances of the imposter distributions, it would adversely influence the genuine distributions. Given two patches of palmprints from the same palm and same location, if we increase the number of filters, the fusion rule has high probability to select different filters for coding. To demonstrate this phenomenon, we match all the palmprints from the same hand. If the fusion rule selects the same filter, the matching distance of these local patches is zero; otherwise it is one. Then, we sum the local matching distances as a global matching distance for comparing two palmprints. The global matching distance is normalized by the matching area as Eq. (11). In other words, we still use hamming distance. Fig. 5(b) shows the cumulative distributions of the genuine hamming distances. We see that the fusion rule using four filters is the easiest to select different filters. When the hamming distance is shorter than 0.3, the fusion rule using three filters performs better than that using two filters. It contradicts our expectation. The reason is that the direction of one of the three filters is close to one of our principal lines. Thus, it provides an extra robustness to the filter selection. Nevertheless, when the hamming distance is longer than 0.3, fusion rule using two filters performs better. This range is more important since false acceptance tends to happen in that region. Combining the influences for the imposter and genuine distributions, the best choice is to employ two filters for fusion. In the following experiments, we study only the two elliptical filters case.

As a side product, we use the fusion rule to select orientation of filters as features and hamming distance as a matching scheme for palmprint verification, exactly the same as the previous discussion. Fig. 5(c) shows the corresponding ROC curves. This figure illustrates that increasing number of filters cannot improve the performance. In addition, the proposed method is better than directly using hamming distance and orientation of filters.

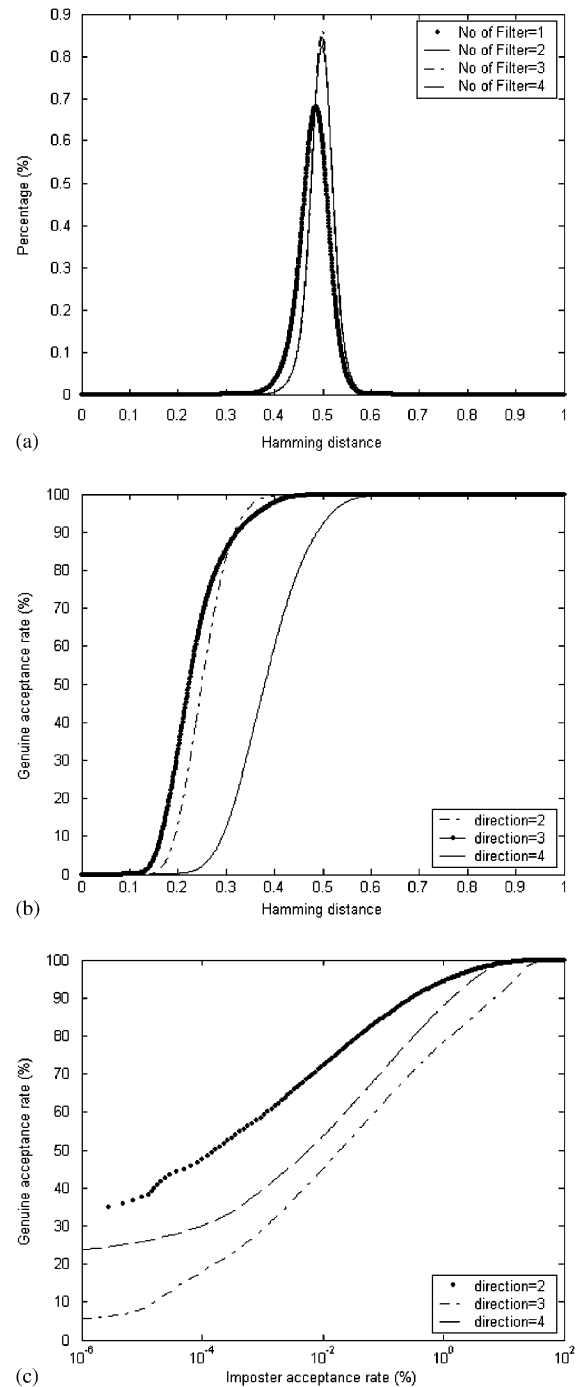


Fig. 5. Analysis of different numbers of filters for fusion. (a) Comparison between imposter distributions using different numbers of elliptical Gabor filters for fusion. (b) The cumulative distributions of hamming distance for studying the fusion rules selecting different filters for coding. (c) The ROC curves of using orientation of the filters as features and hamming distance as a measure.

4.3. Comparison of static and dynamic thresholds

In this experiment, we compare the proposed dynamic threshold and original static threshold. For graphical presentation convenience, we dynamically scale the hamming

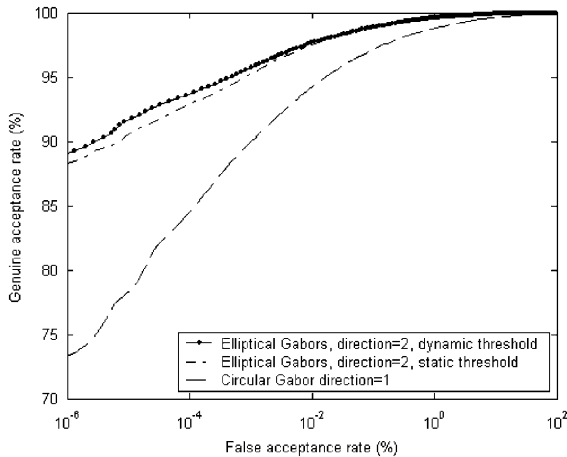


Fig. 6. Comparison between dynamic and static thresholds.

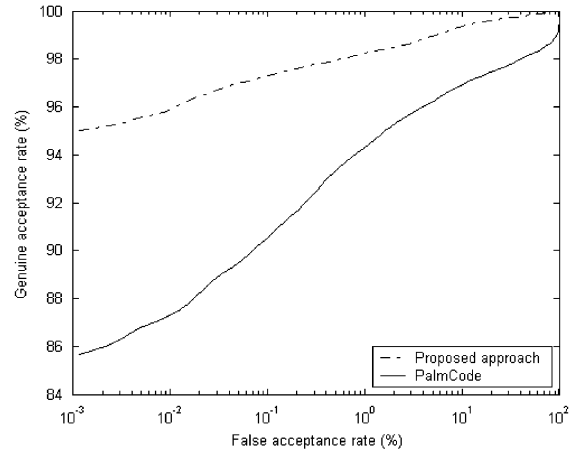


Fig. 7. 1-to-488 identification results.

Table 1
Genuine and false acceptance rates with different threshold values

Threshold	False acceptance rate (%)	False rejection rate (%)
<i>(a) Verification results</i>		
0.317	1.2×10^{-5}	7.77
0.324	1.3×10^{-4}	6.07
0.334	1.0×10^{-3}	4.15
0.350	1.0×10^{-2}	2.32
<i>(b) 1-to-488 identification results</i>		
0.309	6.91×10^{-3}	4.56
0.315	1.38×10^{-2}	3.67
0.323	1.24×10^{-1}	2.61
0.333	9.68×10^{-1}	1.74

distances rather than the threshold. In fact, they have the same effect. Fig. 6 shows their ROC curves. We can see that dynamic threshold effectively improves the accuracy. Combining all the proposed improvements including elliptical Gabor filters, fusion rule and dynamic threshold, the proposed method obtains around 15% improvement for genuine acceptance rate when the false acceptance rate is $10^{-6}\%$. Table 1(a) lists some false acceptance rates and false rejection rates and the corresponding thresholds. The results demonstrate that the proposed method is comparable with the previous palmprint approaches and other hand-based biometric technologies, including hand geometry and fingerprint verification [3,13]. It is also comparable with other fusion approaches [14,15].

4.4. Identification

Identification is a one-against-many, N comparisons process. To establish the identification accuracy of our proposed method, we need to specify N . In the following identification test, we set $N = 488$, which is the total number of different palms in our testing database. Generally, a practical biometric identification system stores several users' templates

in its database for training the system so that the system can recognize noise or deformed signals. Our original testing database is divided into the registering database and the identification database. Three palmprint images collected on the first occasion are selected for the registering database and all the palmprint images collected on the second occasion are put in the identification database. The registering and identification databases contain 1464 and 4821 palmprint images, respectively. Each palmprint image in the identification database is compared with all images in the registering database. Since each palm has three palmprint images in the registering database, each testing image can generate three correct verification hamming distances. The minimum of them is regarded as a correct identification hamming distance. Similarly, each testing image can generate 1461 incorrect verification hamming distances. The minimum of them is regarded as an incorrect identification hamming distance. Thus, both the numbers of the correct and incorrect identification hamming distances are 4821. To obtain more statistically reliable results by generating more incorrect and correct identification hamming distances, we repeated this identification test three times, selecting other palmprint images collected on the first occasion for the registering database. The genuine and imposter identification distributions are generated by 14,463 correct and 14,463 incorrect identification hamming distances, respectively. The corresponding ROC curve is depicted in Fig. 7. As the verification test shown in Fig. 6, we also plot the ROC curve of PalmCode for comparison. Table 1(b) provides the numerical values of false rejection and false acceptance rates with the corresponding thresholds for this test. The ROC curve of Fusion Code and the table show that in 1-to-488 identification, our proposed method can operate at a genuine acceptance rate of 96.33% and the corresponding false acceptance rate is $1.38 \times 10^{-2}\%$. Comparing the two ROC curves, there is no doubt that the proposed Fusion Code is much better than PalmCode.

Table 2
Execution time for our palmprint identification system

Operation	Execution time
Preprocessing	267 ms
Feature extraction	123 ms
Matching	18 μ s

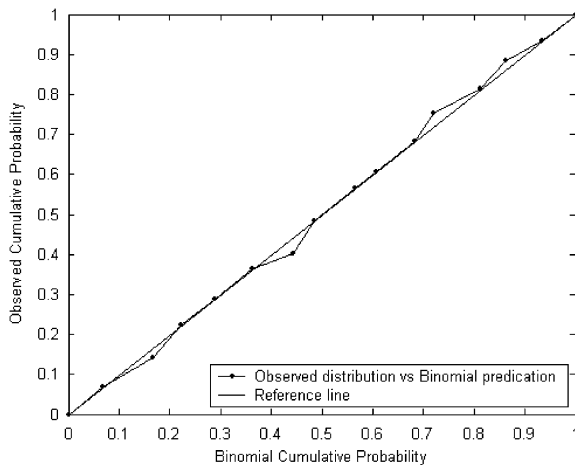


Fig. 8. Plot of the observed cumulative probability versus the predicated binomial cumulative probability.

4.5. Speed

The execution times for the preprocessing, feature extraction and matching are listed in Table 2. These times are estimated using an ASUS notebook embedded Intel Pentium III Mobile processor (933 MHz). The total execution time is about 0.39 s, which is fast enough for real-time verification. For identification, if the database contains 1200 palmprint images for 400 persons, the total identification time is about 0.41 s. In fact, we have not completely optimized the code so it is possible to further reduce the computation time.

5. Discussion on the imposter distribution

In Section 3, we use the assumption that the imposter distribution follows binomial distribution to develop the dynamic threshold. To examine this assumption, we plot the cumulative binomial probabilities against the observed cumulative probabilities. This plot is shown in Fig. 8. If the assumption was valid, the plot would give a straight line, as the reference line in Fig. 8. This figure shows that the observed imposter distribution is close to the binomial distribution in many regions. However, if we use Kolmogorov–Smirnov test to compare the two distributions, the test rejects that they are from the same distribution [16]. Although this assumption is not true, the dynamic threshold still effectively improves the accuracy. Since both IrisCode [11] and Fusion Code use phase information as features and hamming dis-

tance as matching scheme and IrisCode employs binomial distribution to model the imposter distribution of IrisCode [11], some may expect that our imposter distribution also follows binomial distribution. There are two reasons for our imposter distribution following another distribution, not binomial distribution. Ignoring the masks and the normalization constants in Eq. (11), we can formulate the hamming distance as the sum of Bernoulli trails but it does not mean that our imposter distribution follows binomial distribution. A binomial distribution requires another two conditions, stationary and independence. Independence means that all the Bernoulli trails are independent and stationary means that all the Bernoulli trials have the same p , the probability of success. Undoubtedly, matching Fusion Codes cannot fulfill these two conditions. Everyone has principal lines in similar positions so the stationary condition is violated. Moreover, palmprint lines are across several codes so the independence condition is also violated. As a result, our imposter distribution does not follow binomial distribution. Although we can adjust the decision boundaries in Eqs. (7)–(10) to fulfill the stationary condition, our imposter distribution still cannot follow binomial distribution since the sum of correlated Bernoulli trails cannot generate binomial distribution in general [17,18]. Some may further ask why the imposter distribution of IrisCode follows binomial distribution if the sum of correlated Bernoulli trails does not give binomial distribution. If the correlation is first-order stationary Markovian type and the number of trials is large, according to Central limiting Theorem, the distribution follows normal distribution [17,19]. Binomial distribution can be approximated by normal distribution when the degrees-of-freedom is large enough. In terms of application, we totally agree that the imposter distribution of IrisCode follows binomial distribution but in terms of theory, we better say that it follows normal distribution.

6. Conclusion

We have presented a feature-level coding scheme for palmprint identification. On the top of PalmCode [7], we make a number of improvements for developing Fusion Code. (1) The circular Gabor filter in PalmCode is replaced by a bank of elliptical Gabor filters. (2) A feature level fusion scheme is proposed to select a filter output for feature coding. (3) The static threshold in PalmCode is replaced by the dynamic threshold. A series of experiments has been conducted to verify the usefulness of each improvement.

In our testing database containing 9599 palmprint images from 488 different palms, the proposed method achieves around 15% verification improvement for genuine acceptance rate when the false acceptance rate is $10^{-6}\%$. This result is also comparable with those of other hand-based biometrics technologies, such as hand geometry, fingerprint verification and of other fusion approaches. For 1-to-488 identification, our method can operate at a low false

acceptance rate ($1.38 \times 10^{-2}\%$) and a reasonable genuine acceptance rate (96.33%). On a 933 MHz processor, the execution time for the whole process, including preprocessing, feature extraction and final matching, is about 0.4 s.

References

- [1] A. Jain, R. Bolle, S. Pankanti, *Biometrics: Personal Identification in Networked Society*, Kluwer Academic Publishers, Boston, 1999.
- [2] NIST report to the United States Congress, Summary of NIST Standards for Biometric Accuracy, Temper, Resistance, and Interoperability, November 13, 2000.
- [3] R. Sanchez-Reillo, C. Sanchez-Avilla, A. Gonzalez-Marcos, Biometric identification through hand geometry measurements, *IEEE Trans. Pattern Anal. Mach. Intell.* 22 (10) (2000) 1168–1171.
- [4] D. Zhang, W. Shu, Two novel characteristics in palmprint verification: datum point invariance and line feature matching, *Pattern Recognition* 32 (4) (1999) 691–702.
- [5] N. Duta, A.K. Jain, K.V. Mardia, Matching of palmprint, *Pattern Recogn. Lett.* 23 (4) (2001) 477–485.
- [6] C.C. Han, H.L. Cheng, K.C. Fan, C.L. Lin, Personal authentication using palmprint features, *Pattern Recognition* 36 (2) (2003) 371–381.
- [7] D. Zhang, W.K. Kong, J. You, M. Wong, On-line palmprint identification, *IEEE Trans. Pattern Anal. Mach. Intell.* 25 (9) (2003) 1041–1050.
- [8] C.C. Han, A hand-based personal authentication using a coarse-to-fine strategy, *Image Vision Comput.* 22 (2004) 909–918.
- [9] G.M. Lu, D. Zhang, K.Q. Wang, Palmprint recognition using eignpalms features, *Pattern Recogn. Lett.* 24 (2003) 1463–1467.
- [10] L. Zhang, D. Zhang, Characterization of palmprints by wavelet signatures via directional context modeling, *IEEE Trans. Syst. Man Cybern. Part B* 34 (2) (2004) 1335–1347.
- [11] J. Daugman, How iris recognition works, *IEEE Trans. Circuits Syst. Video Technol.* 14 (1) (2004) 21–30.
- [12] A.W.K. Kong, D. Zhang, Feature-level fusion for effective palmprint authentication, in: *Proceedings of the International Conference of Biometric Authentication*, Hong Kong, 15–17 July 2004, pp. 761–767.
- [13] A.K. Jain, S. Prabhakar, L. Hong, S. Pankanti, Filterbank-based fingerprint matching, *IEEE Trans. Image Process.* 9 (5) (2000) 846–859.
- [14] S. Ben-Yacoub, Y. Abdeljaoued, E. Mayoraz, Fusion of face and speech data for person identity verification, *IEEE Trans. Neural Networks* 10 (5) (1999) 1065–1074.
- [15] L. Hong, A.K. Jain, Integrating faces and fingerprints for personal identification, *IEEE Trans. Pattern Anal. Mach. Intell.* 20 (12) (1998) 1295–1307.
- [16] R.V. Hogg, E.A. Tanis, *Probability and Statistical Inference*, fourth ed., Macmillan, New York, 1993.
- [17] K.R. Gabriel, The distribution of the number of success in a sequence of dependent trials, *Biometrika* 46 (1959) 454–460.
- [18] R.W. Katz, Computing probabilities associated with the Markov chain model for precipitation, *J. Appl. Methodol.* 13 (1974) 953–954.
- [19] W. Feller, *An Introduction to Probability Theory and its Applications*, vol. 1, second ed., Wiley, New York, 1957.

About the Author—ADAMS WAI-KIN KONG received his B.Sc. degree in Mathematics from Hong Kong Baptist University with first class honors and obtained his M.Phil. degree from The Hong Kong Polytechnic University. Currently, he studies at University of Waterloo, Canada for his Ph.D. During his study, he received several awards and scholarships from the universities including Scholastic Award, Tuition Scholarships for Research Postgraduate Studies and Graduate Scholarships. Based on his palmprint identification algorithms, he was selected as a finalist of 4th Young Inventor Awards organized by Far Eastern Economic Review and HP invent. He was the only finalist from Hong Kong. He also has patents for these algorithms. The palmprint identification system using his algorithms won a Silver Medal at the Seoul International Invention Fair 2002, Special Gold and Gold Medals at National Invention Exhibition of People Republic of China 2003 and Certificate of Merit from Federation of Hong Kong Industries. His current research interests include biometrics, pattern recognition and image processing.

About the Author—DAVID ZHANG graduated in Computer Science from Peking University in 1974. He received his M.Sc. and Ph.D. in Computer Science and Engineering from the Harbin Institute of Technology (HIT) in 1983 and 1985, respectively. From 1986 to 1988 he was first a Postdoctoral Fellow at Tsinghua University and then an Associate Professor at the Academia Sinica, Beijing. He received his second Ph.D. in Electrical and Computer Engineering from the University of Waterloo, Ontario, Canada, in 1994. Professor Zhang is currently at the Hong Kong Polytechnic University where he is the Founding Director of the Biometrics Technology Centre (UGC/CRC) a body supported by the Hong Kong SAR Government. He also serves as Adjunct Professor in Tsinghua University, Shanghai Jiao Tong University, Harbin Institute of Technology, and the University of Waterloo. He is the Founder and Editor-in-Chief, *International Journal of Image and Graphics (IJIG)*; Book Editor, *Kluwer International Series on Biometrics (KISB)*; Chairman, *Hong Kong Biometric Authentication Society* and Program Chair, the *First International Conference on Biometrics Authentication (ICBA)*, Associate Editor of more than 10 international journals including *IEEE Trans on SMC-A/SMC-C*, *Pattern Recognition*, and is the author of more than 120 journal papers, 20 book chapters and nine books. His research interests include automated biometrics-based authentication, pattern recognition, and biometric technology and systems. Prof. Zhang has won numerous prizes including national, invention and industrial awards and holds a number of patents in both the USA and China. He is currently a Croucher Senior Research Fellow.

About the Author—MOHAMED S. KAMEL received the B.Sc. (Hons) degree in Electrical Engineering from the University of Alexandria, Egypt, in 1970, his M.Sc. degree in Computation from McMaster University, Hamilton, Canada, in 1974 and his Ph.D. degree in Computer Science from the University of Toronto, Canada, in 1981. Since 1985, he has been with the University of Waterloo, Department of Systems Design Engineering and since 2004 in the Department of Electrical and Computer Engineering. He is currently a Canada Research Chair Professor in Cooperative Intelligent Systems and Director of the Pattern Analysis and Machine Intelligence Laboratory. He is the Editor-in-Chief of the *International Journal of Robotics and Automation*, Associate Editor of the *IEEE Trans SMC Part A*, the *Intelligent Automation and Soft Computing*, *Pattern Recognition Letters*, and the *International Journal of Image and Graphics*. He also served as an Associate Editor of *Simulation*, the *Journal of The Society for Computer Simulation*. Prof. Kamel is a member of ACM, AAAI, and IEEE. He has been elevated to a fellow of IEEE starting 2005. He served as a consultant for General Motors, NCR, IBM, Northern Telecom and Spar Aerospace. He is a member of the board of directors and co-founder of Virtek Vision Inc. of Waterloo. His research interests are in computational intelligence, pattern recognition and distributed and multiagent systems. He has authored and co-authored over 200 papers in journals and conference proceedings, two patents and numerous technical and industrial project reports.